Accepted Manuscript

GHz harmonic mode-locking with multi-watts sub-60-fs pulses in a Mamyshev Oscillator

Feihong Qiao, Ze Li, Ning Jia, Xiangtong Zhai, Hao Liang, and Zhiguo Lv*

School of Physical Science and Technology, Research Center for Quantum Physics and Technologies, Inner Mongolia University, Hohhot 010021, China

Abstract Mamyshev oscillator (MO) is well-known for its high modulation depth, which provides an excellent platform for achieving both high average power and short pulse durations. However, this characteristic typically limits the high-repetition-rate pulse generation. Herein, we construct an MO that achieves the gigahertz (GHz) repetition rate through harmonic mode-locking. The laser can reach up to 93rd order that corresponding to the repetition rate of 1.6 GHz. The maximum achieved output average power is 3 W at a repetition rate of 1.2 GHz (69th order), with the corresponding pulse duration compressed to 51 fs. To our knowledge, this is the first time that the GHz repetition rate in MO is obtained simultaneously with the recorded average power and pulse duration.

Key words: gigahertz, high average power, ultrashort pulses

---

*Correspondence to: Zhiguo Lv, School of Physical Science and Technology, Inner Mongolia University, Hohhot 010021, China. Email: lvzhiguo@imu.edu.cn

10.1017/hpl.2025.21

Accepted Manuscript

I. INTRODUCTION

The Mamyshev oscillator (MO), a novel passive mode-locking technique, is frequently employed as an alternative to conventional mode-locking lasers due to its ultra-high modulation depth and exceptional performance in pulse generation [1]. Typically, MO is composed of end-to-end Mamyshev regenerators. And, the mode-locking mechanism relies on the spectral broadening induced by self-phase modulation (SPM) and offset spectral filtering. When the pulse in MO attains sufficient peak power, the spectral broadening induced by SPM effectively bridges the spectral gap between the two filters [2]. With multiple round-trips in the cavity, the pulse is continuously amplified and narrowed. This process results in an intensity-dependent saturable absorber effect. Consequently, this mechanism theoretically enables the MO to attain a 100 % modulation depth, providing a natural advantage in generating high average power and short pulse durations [3-5]. To date, researchers have made significant progress in MO including energy enhancement, pulse shortening, power scaling, and other aspects by utilizing various cavity configurations [6-11]. However, the ultra-high modulation depth also restricts the generation of high repetition rate [12]. It is noteworthy that gigahertz (GHz) repetition rates in MO have not been extensively investigated.

Therefore, how to generate pulses with GHz repetition rate has become a worthwhile research focus in MO. Over the past few decades, two primary methods have been utilized to attain GHz repetition rates. One convenient approach involves shortening the laser cavity length to increase the fundamental frequency [13-17]. Another solution is harmonic mode-locking (HML) [18-21], in which the laser operates at a multiple of its fundamental frequency. For MO, reducing the cavity length to enhance the fundamental frequency presents significant challenges due to its structural configuration, which typically results in a long cavity length. This inherently structural characteristic limits the ability to achieve high repetition rates. Thus, the most effective approach to obtain the high repetition rate in MO is through HML. Under this method, in 2020, Etienne Poeydebat et al. reported the first high-order HML pulse in MO with a repetition of 107.8 MHz [22]. Then, in 2021, a higher HML was achieved with a tunable range of repetition range from 16 to 305 MHz [23]. In 2024, Yu Sui et al. achieved 89^{th} order HML, corresponding to a repetition rate of 395.2 MHz [24]. However, GHz repetition rate in MO has neither been experimentally demonstrated nor

https://doi.org/10.1017/hpl.2025.21 Published online by Cambridge University Press

extensively explored in the literature. This phenomenon can be attributed to the ultra-high modulation depth inherent in MO, which hinders the pulse splitting [12][24]. To attain higher order HML, it is essential to increase the pump power. Nevertheless, as pump power increases, the stability of mode-locking process tends to decrease.

In this work, to decrease the length in MO, the nonlinear polarization rotation （NPR） mechanism is used to initiate MO. The advantage of this approach is that the introduced intensity modulation can significantly broaden the spectrum of the pulse. By adjusting the polarization control device, stable mode-locking can be achieved, allowing the laser to operate independently of long fibers while still obtaining sufficient nonlinear effects. Moreover, the NPR mechanism can enhance the Kerr nonlinear effect in fibers while providing a flexible output coupling ratio. Furthermore, the modulation depth in the MO can be controlled by adjusting the filter separation, thereby minimizing its impact on repetition frequency. Through optimizing filter separation and pump power, GHz HML with high average power and short pulse duration is possible to achieve. In addition, the HML approach reduces the challenges caused by shortening the cavity length to a certain extent.

Based on the above, an MO is constructed, leveraging the NPR mechanism to initiate mode-locking. In the experiment, gain fiber with a 5 μm core diameter is used to enhance the overlap efficiency between the pump source and the gain medium. The smaller core fiber can improve the gain efficiency and amplify the nonlinear effects within the fiber, thereby supporting the higher order HML operation. Additionally, the effect of filter separation on HML is investigated. Notably, the HML order decreases with increasing filter separation, due to the increased modulation depth. A maximum 93rd order HML pulse is realized, corresponding to a repetition rate of 1.614 GHz. By optimizing the filter separation, the laser can generate HML of 69th order, corresponding to a repetition rate of 1.2 GHz, with an average power exceeding 3.1 W. The pulses can be compressed to 51 fs through a grating-pair compressor. Table 1 provides a summary of the HML in MO reported in recent years. To the best of our knowledge, this is the first time to achieve a GHz repetition rate in MO while maintaining high average power and short pulse duration.

https://doi.org/10.1017/hpl.2025.21 Published online by Cambridge University Press

Table 1. Summary of harmonic mode-locking in MO

No.	Fundamental repetition rate (MHz)	Harmonic repetition rate (MHz)	Pulse duration	Average power (W)	SNR (dB)	Refs.
1	7.7	107.8	/	1.3	48	[22]
2	16.3	305	/	/	70	[23]
3	4.45	395.2	3.45 ps	/	60	[24]
4	12.1	48.4	81 fs	0.23	/	[25]
5	7.8	54	1.41 ps	/	45	[26]
6	16.58	116.88	/	/	70	[27]
7	8.84	44.2	/	3.62	/	[28]
8	16	130	7.3 ps	/	40	[29]
9	17.3	1221	51 fs	3.1	60	This work

II. EXPERIMENTAL SETUP

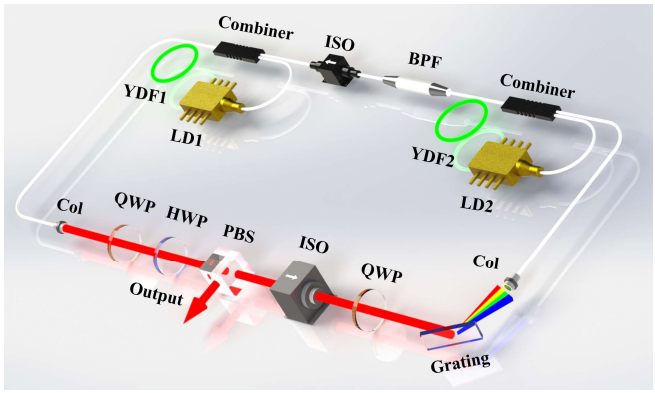

Fig. 1. Schematic setup of MO for generating GHz harmonic mode-locking. Col, collimators; YDF, Yb-doped fiber; BPF, bandpass filter; QWP, quarter-wave plate; HWP, half-wave plate; PBS, polarization beam splitters; ISO, isolator. LD, laser diode.

As illustrated in Fig. 1, in the first arm, a 1.5 m long ytterbium-doped double-clad fiber (YDF 2, Yb1200-10/125, LIEKKI) is used as a gain medium. The gain fiber is co-pumped by multimode laser diodes with power up to 9 W at 976 nm through fusion spliced combiners. For easy control and adjustment in filter separation ($\Delta\lambda_f$), a 600 lines/mm reflection grating in combination with a collimator is used as a variable spectra filter (grating filter), and the 3 dB bandwidth is 2.3 nm. By moving the collimator, the transmitted central wavelength of the grating filter could be tuned from

https://doi.org/10.1017/hpl.2025.21 Published online by Cambridge University Press

1040 nm to 1047 nm. This adjustment leads to an increment in $\Delta\lambda_f$ between the two filters. In the second arm, the gain fiber (YDF 1, Yb1200-5/130, LIEKKI) is 4.5 meters long and is pumped by a multimode laser diode with power up to 27 W. The central wavelength of the bandpass filter (BPF) is 1040 nm with a 3 dB bandwidth of 3 nm. An NPR configuration is constructed to initial the laser. It incorporates a pair of quarter-wave plates, a half-wave plate, and a polarization beam splitter. Two isolators are incorporated in the cavity to ensure the unidirectional oscillation. The output pulses are subsequently dechirped using a grating compressor composed of two transmission gratings (1000 lines/mm).

III. RESULTS

To initiate the MO, it is essential to overlap the two filters so that the low-peak-power noise can be easily transmitted in the cavity, thereby initiating mode-locking [30]. Consequently, the center wavelength of the grating filter is tuned to 1040 nm to match that of the BPF, resulting in a $\Delta\lambda_f$ at 0 nm. By rotating the plates between the two arms, the initial mode-locking pulses can be achieved under the NPR mechanism. The corresponding pump power emitted from LD 1 and LD 2 are 1.25 W and 1.64 W, respectively. Once mode-locking is initiated, the stable mode-locking operation can be sustained by increasing pump power and adjusting the output coupling ratio. As the $\Delta\lambda_f$ increases to 3 nm, a mode-locking state characterized by a sudden broadening spectrum (as shown in Fig.2 (a)) is obtained. This phenomenon indicates the genuine transition of the laser into the MO mechanism. Fig. 2(b) presents the measured pulse train with an interval of 57.6 ns, corresponding to the fundamental repetition rate of 17.36 MHz. The radio frequency (RF) spectrum around this fundamental repetition rate is illustrated in Fig. 2(c), showing a SNR up to 73 dB.

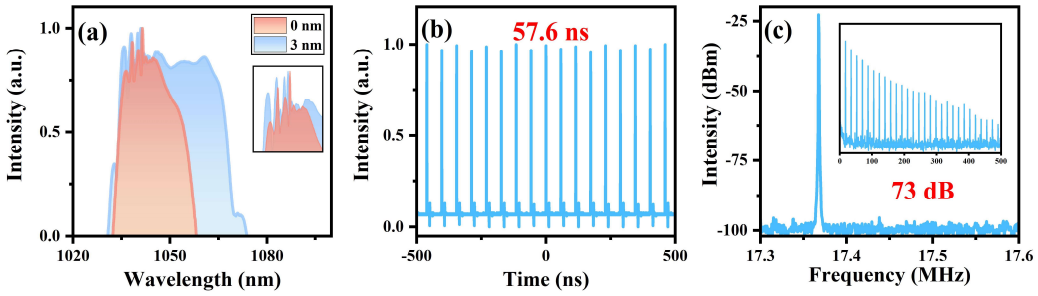

https://doi.org/10.1017/hpl.2025.21 Published online by Cambridge University Press

FIG. 2. Experiment results. (a) spectra: red is the mode-locked spectrum when the $\Delta\lambda_f$ is 0 nm; blue is the mode-locked spectrum when the $\Delta\lambda_f$ is 3 nm; inset: zoom-in of the CW state. (b) pulse train. (c) RF spectrum.

With further increasing pump power, multiple pulses emerge in the cavity due to the energy quantization. These pulses can either form a tight packet or be distributed randomly throughout the cavity [31]. Then, the polarization and pump power need to be carefully controlled to balance the gravitational and repulsive forces between adjacent pulses. This balance results in pulse envelope at equal intervals, enabling the pulses to operate in burst mode. Furthermore, the number of pulses in the packet can be increased by enhancing the pump power. To further explore the characteristics of these pulse bursts, the evolution of the output parameters is measured. As shown in Fig. 3, the pulse envelope gradually broadens, with widths ranging from 0.13 to 0.53 ns as the pump power increases. This broadening is attributed to intensified pulse splitting, which results in growing sub-pulses, thereby expanding the overall envelope. However, due to the bandwidth limitations of the oscilloscope, accurately measuring the number of sub-pulses and their intervals within the burst is not feasible. It is also noteworthy that the intervals between pulses are not uniform, which may be attributed to random dispersive waves. Additionally, in multi-pulse regimes, as pump power increases, the pulse interaction rises. The intensity of one pulse can affect the phase of another, potentially leading to asymmetric pulse profiles and splitting. Furthermore, weak intensity fluctuations may arise from competition between adjacent pulses. The occurrence of the above phenomenon offers a promising approach for generating GHz pulses by effectively managing nonlinearity, gain, and output coupling ratio.

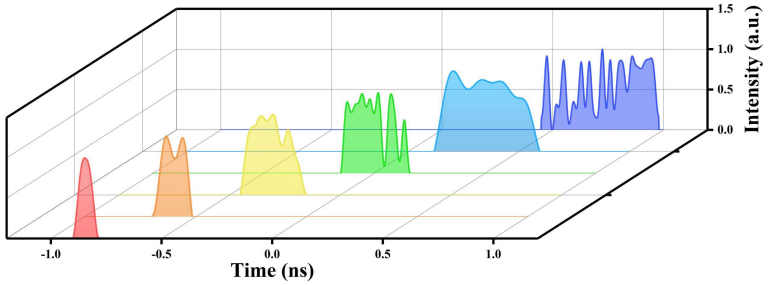

FIG. 3. Evolution of the pulses as increasing pump powers

Subsequently, as the pump power continues to increase, slight adjustments are made to the polarization within the cavity by rotating the QWP and HWP. This introduced disturbance disrupts the balance between gain and loss, leading to the

https://doi.org/10.1017/hpl.2025.21 Published online by Cambridge University Press

disappearance of the burst mode. Simultaneously, numerous pulses emerge, exhibiting randomly distributed intervals among the sub-pulses. Through the optimization of polarization to balance the repulsion and attraction between sub-pulses, a novel operational regime has been observed [32]. In this case, the intervals between adjacent pulses become uniform, allowing the laser to achieve HML operation. As the pump power is continuously increased, Fig. 4 illustrates the output pulse trains for various orders of HML operation: 11th order (191 MHz), 14th order (243 MHz), 35th order (607 MHz), 45th order (781 MHz), 51st order (885 MHz), and 59th order (1024 MHz) HML. The interval between adjacent harmonic pulses is 5.237 ns, 4.115 ns, 1.647 ns, 1.280 ns, 1.130 ns, and 0.976 ns respectively, which are the reciprocals to repetition frequency. The insets of Fig. 4. reveal the SNRs of the HML pulses, respectively, which can confirm stable HML operation. Consequently, in MO, GHz mode-locking can be achieved by the HML approach.

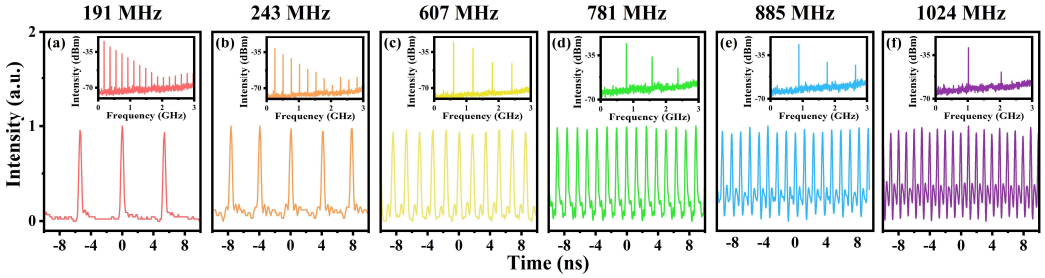

FIG. 4. HML pulses train and RF spectrum. (a) 11th. (b) 14th. (c) 35th. (d) 45th. (e) 51st. and (f) 59th harmonic orders.

Due to the mechanism of MO, the modulation depth increases as the increment in $\Delta\lambda_f$, resulting in enhanced output performance. To improve output performance, the relationship between $\Delta\lambda_f$ and the generation of GHz is further investigated. Fig. 5 presents the pulse train with the maximum achievable HML repetition rate under different $\Delta\lambda_f$, along with the corresponding spectra. As $\Delta\lambda_f$ and pump power increase, the spectra exhibit broadening and red-shifting. Interestingly, Fig. 5 reveals that the maximum order of HML decreases as $\Delta\lambda_f$ increases, declining from an initial 1.614 GHz to 0.972 GHz. This phenomenon is hypothesized to result from the increasing modulation depth in MO as the $\Delta\lambda_f$ increases. Although sufficient modulation depth enables the production of a broader spectrum, it simultaneously impedes pulse splitting, thereby obstructing the generation of GHz. Additionally, further increment in pump

https://doi.org/10.1017/hpl.2025.21 Published online by Cambridge University Press

power can disrupt mode-locking, when the modulation depth becomes larger. Thus, In MO lasers, there exists an inherent contradiction between achieving a high repetition frequency and spectral broadening, which corresponds to a shortened pulse duration. Consequently, it is essential to establish a balance between these factors to determine the optimal operating parameters. Achieving this balance allows for the simultaneous achievement of high repetition frequencies, high average power, and short pulse duration.

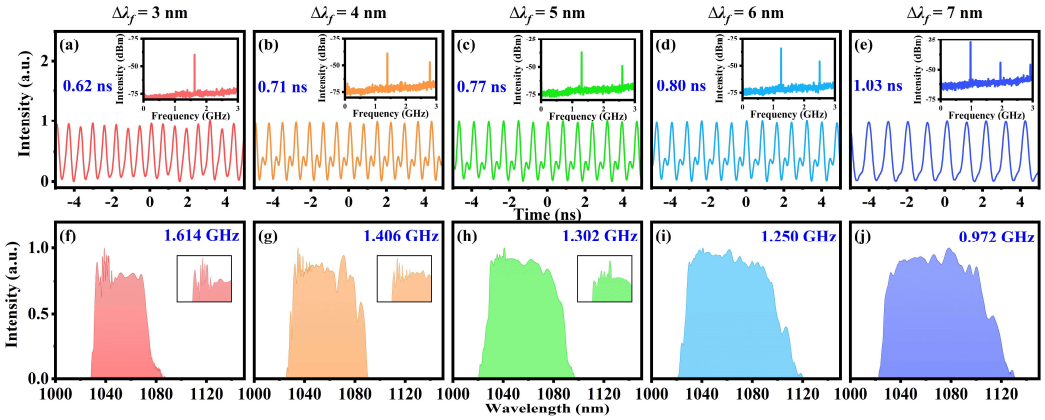

FIG. 5. Experiment results under different $\Delta\lambda_f$. (a-e) pulse train, inset: RF spectrum. (f-j) spectra, inset: zoom-in of the CW state.

In MO, the continuous wave (CW) component in spectra can, to some extent, reflect the intensity of modulated depth. Insufficient modulation depth fails to suppress the CW component, leading to a pronounced CW peak at 1040 nm, as shown in Fig. 2(a) and 5(f). As $\Delta\lambda_f$ increases, the modulation depth becomes larger, gradually suppressing the CW continuous wave, as illustrated in Fig. 5(g-j). Notably, when $\Delta\lambda_f$ reaches 7 nm, the CW component is fully suppressed, indicating a higher modulation depth. Although this allows for a wider spectrum, it also reduces the harmonic order. Consequently, maintaining the GHz harmonic mode-locked state becomes difficult when $\Delta\lambda_f$ is over 7 nm.

Table 2. Output of harmonic mode-locking in this MO

No.	$\Delta\lambda_f$ (nm)	Harmonic repetition rate (MHz)	Spectral Width (nm)	Average power (W)
1	3.0	1614	40	1.1
2	4.0	1406	49	1.3
3	5.0	1302	53	1.8

https://doi.org/10.1017/hpl.2025.21 Published online by Cambridge University Press

4	5.5	1280	63	2.1
5	6.0	1250	67	2.4
6	6.5	1200	71	3.1
7	7.0	972	75	3.4

Based on the insights obtained from the previous experiments, further optimization of the laser parameters is conducted. Table 2 summarizes the spectral widths and average output power in various $\Delta\lambda_f$. Specifically, setting the $\Delta\lambda_f$ to 6.5 nm enables the laser to meet the requirements for high repetition frequency, high average power, and wider Spectrum. The specific tests are as follows: the central wavelength of the grating filter is adjusted to 1046.5 nm. As the pump power is increased, the QWP and HWP are slightly rotated to adjust the output coupling ratio. When pump power from LD 1 and LD 2 are set to 15.4 W and 8.7 W, respectively, the maximum HML repetition rate is obtained, as seen in Fig. 6(a) The interval between adjacent pulses is 0.833 ns, corresponding to a repetition rate of 1.2 GHz (69th order). Fig. 6 presents the detailed characteristics of the pulses with a repetition rate of 1.2 GHz. The SNR, as shown in the inset, indicates stable operation in the laser. The output spectrum is depicted in Fig. 6(b), with a central wavelength is 1051 nm and a 10 dB bandwidth of 71 nm. As illustrated in Fig. 6(c), after compression, the pulse duration is reduced to 51 fs. The pulse has a small amount of pedestal structure, which we estimate to comprise less than 10 % of the pulse energy. Under optimum parameters, the maximum output average power is 3.1 W. To the best of our knowledge, this is the first time a GHz repetition rate in MO has been achieved while maintaining a Watt-level average power and short pulse duration.

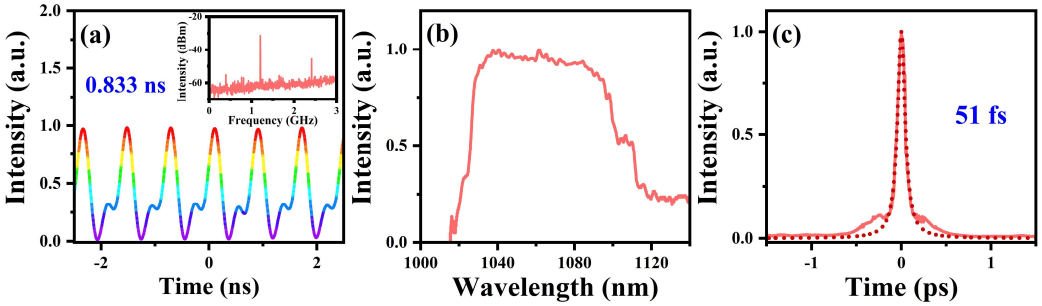

FIG. 6. Experimental results. (a) pulse train; inset: RF spectrum. (b) spectrum. (c) autocorrelation trace.

The stability of the MO is also assessed at the maximum average power. The output average power is continuously monitored and recorded at one-second intervals,

https://doi.org/10.1017/hpl.2025.21 Published online by Cambridge University Press

with the results presented in Fig. 7. The root mean square (RMS) fluctuation of the recorded power values is calculated to be less than 0.30%, indicating a high level of power stability.

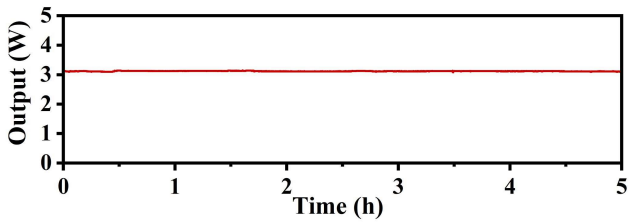

FIG. 7. Power stability measurement of the mode-locked MO within 5 hours.

IV. CONCLUSION

In conclusion, we construct an MO capable of achieving a GHz repetition rate through HML. The MO utilizes the NPR mechanism in conjunction with a gain fiber featuring a 5 μm core diameter. This configuration enhances gain efficiency and amplifies nonlinear effects, thereby facilitating higher-order harmonic mode-locking operations. Notably, the HML order decreases with increasing filter separation due to increased modulation depth. A maximum HML order of 93rd is obtained, corresponding to a repetition rate of 1.6 GHz. By optimizing the filter separation, the laser is able to generate pulses at a repetition rate of 1.2 GHz (69th order), with an average power exceeding 3 W. The pulses are compressed to 51 fs using a grating-pair compressor. Fig. 8 provides a summary of the GHz harmonic mode-locking reported in recent years. To the best of our knowledge, these results represent the highest average power and shortest pulse duration in the field of GHz harmonic mode-locking.

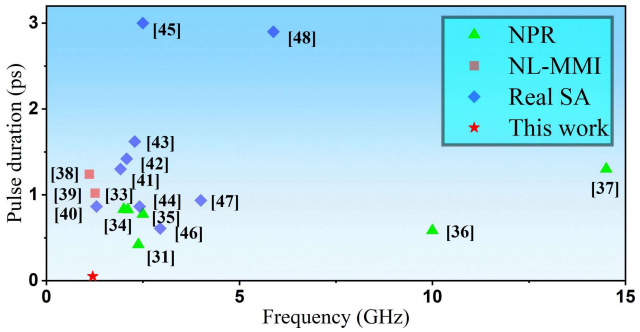

FIG. 8. Overview of GHz harmonic mode-locking in different configurations

https://doi.org/10.1017/hpl.2025.21 Published online by Cambridge University Press

Accepted Manuscript

Acknowledgment

National Natural Science Foundation of China (NSFC) (12164030); Young Science and Technology Talents of Inner Mongolia (NJYT22101); The Central Government Guides Local Science and Technology Development Fund Projects (2023ZY0005); Science and Technology Plan Projects of Inner Mongolia Autonomous Region of China (Grant No. 2023KYPT0012).

References

[1]. Y. Y. Li, B. Gao, C. Y. Ma, G. Wu, J. Y. Huo, Y. Han, S. Wageh, Q. A. AI-Hartomy, A. G. AI-Sehemi, L. Liu, and H. Zhang, "Generation of High-Peak-Power Femtosecond Pulses in Mamyshev Oscillator: Recent Advances and Future Challenges," Laser Photonics Rev. **17**(4), 2200596 (2023). DOI: https://doi.org/10.1002/lpor.202200596

[2]. H. Haig, P. Sidorenko, R. Thorne, and F. Wise, "Megawatt pulses from an all-fiber and self-starting femtosecond oscillator," Opt. Lett. **47**(4), 762-765 (2022). DOI: https://doi.org/10.1364/OL.450313

[3]. M. Rochette, L. R. Chen, K. Sun, and J. Hernandez-Cordero, "Multiwavelength and tunable self-pulsating fiber cavity based on regenerative SPM spectral broadening and filtering," IEEE Photonics Technol. Lett. **20**(17), 1497–1499 (2008). DOI: https://doi.org/10.1109/LPT.2008.928531

[4]. T. North and M. Rochette, "Regenerative self-pulsating sources of large bandwidths," Opt. Lett. **39**(1), 174–177 (2014). DOI: https://doi.org/10.1364/OL.39.000174

[5]. J. C. Zheng, S. Yang, K. Y. Lau, Z. W. Zhu, L. Li, "Recent research progress of Mamyshev oscillator for high energy and ultrashort pulse generation," Opt. Fiber Technol. **67**,102691 (2021). DOI: https://doi.org/10.1016/j.yofte.2021.102691

[6]. V. Boulanger, M. Olivier, B. Morasse, F. Trépanier, M. Bernier, and M. Piché, "Femtosecond Mamyshev oscillator at 920 nm,". Opt. Lett. **49**(8), 2201-2204 (2024). DOI: https://doi.org/10.1364/OL.522902

[7]. H. Xu, C. X. Zhang, D. Y. Fan, C. Y. Ma, P. H. Tang, and J. Liu, "Generation of ultrashort cylindrical vector beams from a Mamyshev oscillator," Opt. Lett. **49**(21), 6121-6124 (2024). DOI: https://doi.org/10.1364/OL.537261

[8]. V. Boulanger, M. Olivier, F. Trépanier, P. Deladurantaye, and M. Piché1, "Multi-megawatt pulses at 50 MHz from a single-pump Mamyshev oscillator gain-managed amplifier laser," Opt. Lett. **48**(10), 2700-2703 (2023). DOI:

https://doi.org/10.1364/OL.490075

[9]. D. Lin, D. Xu, J. He, Y. Feng, Z. Ren, R. Sidharthan, Y. Jung, S. Yoo, D. J. Richardson, "The generation of 1.2 μJ pulses from a Mamyshev oscillator based on a high concentration, large-mode-area Yb-doped fiber," J. Lightwave Technol. **40**(21), 7175-7179 (2022). DOI: https://doi.org/10.1109/JLT.2022.3198737

[10]. C. Y. Ma, A. Khanolkar, Y. Zang, and A. Chong, "Ultrabroadband, few-cycle pulses directly from a Mamyshev fiber oscillator," Photonics Res. **8**(1), 65-69 (2020). DOI: https://doi.org/10.1364/PRJ.8.000065

[11]. M. Nie, J. Wang, and Shu Wei. Huang, "Solid-state Mamyshev oscillator." Photonics Res. **7**(10), 1175-1181 (2019). DOI: https://doi.org/10.1364/PRJ.7.001175

[12]. J. Želudevičius, M. Mickus, and K. Regelskis, "Investigation of different configurations and operation regimes of fiber pulse generators based on nonlinear spectral re-shaping," Opt. Express, **26**(21) 27247– 27264, (2018). DOI: https://doi.org/10.1364/OE.26.027247

[13]. J. J. McFerran, L. Nenadović, W. C. Swann, J. B. Schlager, and N. R. Newbury, "A passively mode-locked fiber laser at 1.54 μm with a fundamental repetition frequency reaching 2 GHz," Opt. Express, **15**(20), 13155–13166, (2007). DOI: https://doi.org/10.1364/OE.15.013155

[14]. Y. W. Song, S. Yamashita, C. S. Goh, and S. Y. Set, "Passively mode-locked lasers with 17.2-GHz fundamental-mode repetition rate pulsed by carbon nanotubes," Opt. Lett. **32**(44), 430–432, (2007). DOI: https://doi.org/10.1364/OL.32.000430

[15]. S. Kimura, S. Tani, and Y. Kobayashi, "Kerr-lens mode locking above a 20 GHz repetition rate," Optica, **6**(5),532-533 (2019). DOI: https://doi.org/10.1364/OPTICA.6.000532

[16]. L. Zheng, W. L. Tian, H. C. Xue, Y. H. Chen, G. Y. Wang, C. Bai, Y. Yu, Z. Y. Wei, and J. F. Zhu "Diode-pumped high-power gigahertz Kerr-lens mode-locked solid-state oscillator enabled by a dual-confocal ring cavity," High Power Laser Sci. Eng. **12**, 66 (2024). DOI: https://doi.org/10.1017/hpl.2024.42

[17]. C. J. Zhu, X. Z. Yang, Y. X. Liu, M. Y. Li, Y. X, Sun, J. J. Fang, D. J. Chen, W. B. Chen, Y. Feng, "GHz-level repetition rate synchronously pumped diamond Raman laser based on bidirectional gain," Appl. Phys. Lett. **125**, 4 (2024). DOI: https://doi.org/10.1063/5.0217381

[18]. G. Sobon, J. Sotor, K. M. Abramski, "Passive harmonic mode-locking in Er-doped fiber laser based on graphene saturable absorber with repetition rates scalable to 2.22 GHz," Appl. Phys. Lett. **100**, 16 (2012). DOI: https://doi.org/10.1063/1.4704913

https://doi.org/10.1017/hpl.2025.21 Published online by Cambridge University Press

[19]. S. Tao, L. Xu, G. Chen, C. Gu, and H. Song, “Ultra-high repetition rate harmonic mode-locking generated in a dispersion and nonlinearity managed fiber laser,” J. Lightwave Technol. **34**(9), 2353– 2356, (2016). DOI: https://doi.org/10.1109/JLT.2016.2528304

[20]. M. Pang, W. He, and P. St. J. Russell. "Gigahertz-repetition-rate Tm-doped fiber laser passively mode-locked by optoacoustic effects in nanobore photonic crystal fiber." Opt. Lett. **41**(19), 4601-4604, (2016). DOI: https://doi.org/10.1364/OL.41.004601

[21]. Y. D. Ling, Q. Q, Huang, C. H. Zou, Z. K. Xing, Z. J. Yan, C. Zhao, K. M. Zhou, L. Zhang, and C.B. Mou, “L-Band GHz Femtosecond Passively Harmonic ModeLocked Er-Doped Fiber Laser Based on Nonlinear Polarization Rotation,” IEEE Photonics J. **11**(4), 1–7, 2(2019). DOI: https://doi.org/10.1109/JPHOT.2019.2927771

[22]. E. Poeydebat, F. Scol, O. Vanvincq, G. Bouwmans, and E. Hugonnot, "All-fiber Mamyshev oscillator with high average power and harmonic mode-locking," Opt. Lett. **45**(6), 1395-1398 (2020). DOI: https://doi.org/10.1364/OL.389522

[23]. B. Piechal, J. Szczepanek, T. M. Karda´s, and Y. Stepanenko, "Mamyshev oscillator with a widely tunable repetition rate," J. Lightwave Technol. **39**(2), 574-581 (2021). DOI: https://doi.org/10.1109/JLT.2020.3031540

[24]. Y. Sui, L. Jin, Y. K. Liu, H. Zhang, and Y. T. Xu, "Harmonic Mode-Locking from Erbium-Doped Fiber Self-Starting Mamyshev Oscillator," J. Lightwave Technol. **42**(5), 1605-1610 (2024). DOI: https://doi.org/10.1109/JLT.2023.3325270

[25]. Y. Q, Sun, Y. Z, Zhou, Y. Z. Hou, Y. M. Liu, T. Luo, Z. L. Li, B. Q Li, T. S. Wang, X. J. Pan. "41.6 nm/44 fs Mamyshev Yb-doped fiber laser with bound-state solitons and multiple harmonics," Opt. Commun. **574**, 131221 (2025). DOI: https://doi.org/10.1016/j.optcom.2024.131221

[26]. J. Liu, C. Wang, X. Li, M. Han, and S. Zhang, “Pulse buildup dynamics in a self-starting Mamyshev oscillator,” Opt. Express, **32**(4), 5851-5861 (2024). DOI: https://doi.org/10.1364/OE.515557

[27]. T. Qiu, F. H. Qiao, B. L. Song, X. Li, X. H. Dou, S. Wang, and Z.G. Lv "Enhanced nonlinear effect for generation of both bound state solitons and harmonic mode-locking with high signal-to-noise ratio based on crossed bandpass transmittance filters," J. Lightwave Technol. **42**(15),5337-5342 (2024). DOI: https://doi.org/10.1109/JLT.2024.3389934

[28]. T. Wang, C. Li, B. Ren, K. Guo, J. Wu, J. Y. Leng, and P. Zhou. "Time jitter and intensity noise of an all-fiber high-power harmonic Mamyshev oscillator," J. Lightwave Technol. **41**(19), 6369-6373 (2023). DOI: https://doi.org/10.1109/JLT.2023.3278678

https://doi.org/10.1017/hpl.2025.21 Published online by Cambridge University Press

[29]. D. Yan, X. Li, S. Zhang, and J. Liu, “Pulse dynamic patterns in a self-starting Mamyshev oscillator,” Opt. Express **29**(7), 9805-9815 (2021). DOI: https://doi.org/10.1364/OE.419948

[30]. S. Pitois, C. Finot, L. Provost, and D. J. Richardson, “Generation of localized pulses from incoherent wave in optical fiber lines made of concatenated Mamyshev regenerators,” J. Opt. Soc. Am. B **25**(9), 1537–1547 (2008). DOI: https://doi.org/10.1364/JOSAB.25.001537

[31]. X. L. Li, S. M. Zhang, Y. P. Hao, and Z. J. Yang. "Pulse bursts with a controllable number of pulses from a mode-locked Yb-doped all fiber laser system," Opt. Express, **22**(6), 6699-6706 (2014). DOI: https://doi.org/10.1364/OE.22.006699

[32]. X. M. Liu, and M. Pang. "Revealing the buildup dynamics of harmonic mode-locking states in ultrafast lasers," Laser Photonics Rev. **13**(9), 1800333 (2019). DOI: https://doi.org/10.1002/lpor.201800333

[33]. M. Pang, X. Jiang, W. He, G. K. L. Wong, G. Onishchukov, N. Y. Joly, G. Ahmed, C. R. Menyu, and P. ST. J. Russell. "Stable subpicosecond soliton fiber laser passively mode-locked by gigahertz acoustic resonance in photonic crystal fiber core," Optica **2**(4), 339-342 (2015). DOI: https://doi.org/10.1364/OPTICA.2.000339

[34]. D. H. Yeh, W. B. He, M. Pang, X. Jiang, G. Wong, and PHILIP ST.J. Russell. "Pulse-repetition-rate tuning of a harmonically mode-locked fiber laser using a tapered photonic crystal fiber,"Opt. Lett. **44**(7), 1580-1583 (2019). DOI: https://doi.org/10.1364/OL.44.001580

[35]. Z. H. Zhao, L. Jin, Sze Yun Set, and S. J. Yamashita. "2.5 GHz harmonic mode locking from a femtosecond Yb-doped fiber laser with high fundamental repetition rate," Opt. Lett. **46**(15), 3621-3624 (2021). DOI: https://doi.org/10.1364/OL.431735

[36]. X. X. Zhou, Y. Zhou, W. J. Wang, T. Zhang, and K. Xu. "Generation of 583 fs optical pulses at 10 GHz from a regeneratively mode-locked fiber laser combining nonlinear polarization evolution," Opt. Express, **32**(5), 6977-6985 (2024). DOI: https://doi.org/10.1364/OE.515029

[37]. Y. Z. Wang, J. F. Li, K. D. Mo, Y. Y. Wang, F. Liu, and Y. Liu, "14.5 GHz passive harmonic mode-locking in a dispersion compensated Tm-doped fiber laser," Sci. Rep. **7**(1), 7779 (2017). DOI: https://doi.org/10.1038/s41598-017-06326-5

[38]. S. Wang, X. Li, X. H. Li, Y. Li, J. T. Qiu, B. L. Song, X. H. Dou, F. H. Qiao, and Z. G. Lv, "Route to L-Band GHz Nonlinear Multimodal Interference Mode-Locked Fiber Laser," J. Lightwave Technol. **42**(15), 5330-5336 (2024). DOI: https://doi.org/10.1109/JLT.2024.3388477

[39]. X. H. Li, L. Jin, R.Y. Wang, S. Z. Xie, X. C. Zhang, H. Zhang, Y. T. Xu, X. H. Ma, "GHz-level all-fiber harmonic mode-locked laser based on microfiber-assisted nonlinear multimode interference," Opt. Laser Technol. **155**, 108367 (2022). DOI:

https://doi.org/10.1017/hpl.2025.21 Published online by Cambridge University Press

https://doi.org/10.1016/j.optlastec.2022.108367

[40]. J. Lee, S.Y. Kwon, J. H. Lee "Harmonically mode-locked Er-doped fiber laser at 1.3 GHz using a V2AlC MAX phase nanoparticle-based saturable absorber," Opt. Laser Technol. **145**, 10752, (2022). DOI: https://doi.org/10.1016/j.optlastec.2021.107525

[41]. X. H. Li, Y. H. Han, Z. J. Shi, M. Q. An, E. C. Chen, J. J. Feng, and Q. J. Wang, "β-In2S3 nanoplates for ultrafast photonics," ACS Appl. Nano Mater. **5**(3), 3229-3236 (2022). DOI: https://doi.org/10.1021/acsanm.1c03542

[42]. Q. Q. Huang, C. H. Zou, T. X, Wang, M. A. Araimi, A. Rozhin, and C. B. Moul, "Influence of average cavity dispersion and spectral bandwidth on passively harmonic mode locked L-band Er-doped fiber laser," IEEE J. Sel. Top. Quantum Electron. **25**(4), 1-8 (2019). DOI: https://doi.org/10.1109/JSTQE.2019.2924869

[43]. Y. J. Wang, C. Y. Song, H. Zhang, L. Jin, Y. T. Xu, Y. G. Zou, and X. H, Ma, "Study on the relationship between carrier mobility and nonlinear optical characteristics of Sb 2 Te 3–Bi 2 Te 3 lateral heterostructure materials and its applications in fiber lasers," J. Mater. Chem. C **10**(33), 11862-11873 (2022). DOI: https://doi.org/10.1039/D2TC01677J

[44]. Q. Q. Huang, Z. N. Huang, M. A. Araimi, A. Rozhin, and C. B. Mou, "2.4 GHz L-band passively harmonic mode locked Er-doped fiber laser based on carbon nanotubes film," IEEE Photonics Technol. Lett. **32**(2), 121-124 (2019). DOI: https://doi.org/10.1109/LPT.2019.2960112

[45]. M. Liu, X. W. Zheng, Y. L. Qi, H. Liu, A. P. Luo, Z. C. Luo, W. C. Xu, C. J. Zhao, and H. Zhang, "Microfiber-based few-layer MoS 2 saturable absorber for 2.5 GHz passively harmonic mode-locked fiber laser," Opt. Express, **22**(19), 22841-22846 (2014). DOI: https://doi.org/10.1364/OE.22.022841

[46]. P. G. Yan, R. Y. Lin, S. C. Ruan, A. J. Liu, and H. Chen, "A 2.95 GHz, femtosecond passive harmonic mode-locked fiber laser based on evanescent field interaction with topological insulator film," Opt. Express, **23**(1), 154-164 (2015). DOI: https://doi.org/10.1364/OE.23.000154

[47]. Q. Q. Huang, L. L. Dai, A. Rozhin, M. A. Araimi, and C. B. Mou. "Nonlinearity managed passively harmonic mode-locked Er-doped fiber laser based on carbon nanotube film," Opt. Lett. **46**(11), 2638-2641 (2021). DOI: https://doi.org/10.1364/OL.425898

[48]. Y. C. Meng, A. Niang, K. Guesmi, M. Salhi, and F. Sanchez, "1.61 μm high-order passive harmonic mode locking in a fiber laser based on graphene saturable absorber," Opt. Express, **22**(24), 29921-29926 (2014). DOI: https://doi.org/10.1364/OE.22.029921

https://doi.org/10.1017/hpl.2025.21 Published online by Cambridge University Press